Photo-Oxidative Stability of Recycled Polypropylene: Effect of a Repair Additive on Degradation and Mechanical Retention

applied sciences

MDPI

Article

Photo-Oxidative Stability of Recycled Polypropylene: Effect of a Repair Additive on Degradation and Mechanical Retention

Giulia Bernagozzi [1,2], Rossella Arrigo [1,2,*] and Alberto Frache [1,2]

[1] Department of Applied Science and Technology, Politecnico di Torino, Viale Teresa Michel 5, 15121 Alessandria, Italy; giulia.bernagozzi@polito.it (G.B.); alberto.frache@polito.it (A.F.)
[2] Consorzio Interuniversitario Nazionale per la Scienza e Tecnologia dei Materiali (INSTM), Via G. Giusti 9, 50121 Florence, Italy
* Correspondence: rossella.arrigo@polito.it

Abstract

The increasing use of recycled polypropylene (rPP) in technical and outdoor applications requires strategies to limit photo-oxidative degradation while maintaining adequate performance after reprocessing. In this work, the photo-oxidative stability of rPP films was investigated under accelerated weathering conditions, focusing on the effect of a commercially available additive, Nexamite® R201 (NEX), previously shown to partially restore PP molecular weight after reprocessing. Films of rPP and rPP containing 5 wt.% NEX were produced by cast extrusion and exposed to cyclic UVA irradiation and water condensation in a QUV chamber, and the evolution of the functional and structural degradation of the materials was monitored as a function of aging time. Spectroscopical analyses showed progressive oxidation in both systems, with carbonyl growth starting after an induction period of about 200 h. A faster increase in the carbonyl index was observed for rPP containing NEX, indicating that the additive does not improve chemical oxidative resistance under the adopted conditions. However, NEX significantly enhanced the retention of mechanical properties during aging, with higher elongation and stress at break compared with unmodified rPP, thus delaying embrittlement. Overall, the results show that the investigated additive effectively mitigates the loss of mechanical integrity during photo-aging, likely as a consequence of the macromolecular restructuring induced during reprocessing.

Keywords: mechanical recycling; post-consumer recycling; photo-oxidative degradation; molecular weight rebuilding; long-term stability

1. Introduction

Polypropylene (PP) is one of the most widely used polyolefins due to its low cost, ease of processing, and balanced mechanical properties, finding extensive application in packaging, automotive components, and consumer goods [1,2]. In recent years, the increasing demand for sustainable materials and the implementation of circular economy strategies have significantly boosted the use of recycled polypropylene (rPP), particularly in non-food and technical applications [3,4]. However, the reuse of rPP is often limited by the degradation phenomena accumulated during its service life and recycling processes, which lead to a reduced molecular weight, altered macromolecular architecture, and deteriorated mechanical performance [5]. These limitations are especially critical when rPP is intended for outdoor applications, where prolonged exposure to ultraviolet (UV) radiation, oxygen, and moisture accelerates photo-oxidative degradation.

Academic Editor: Paulo Santos

Received: 9 April 2026
Revised: 29 April 2026
Accepted: 8 May 2026
Published: 11 May 2026

Photo-oxidative aging of polypropylene involves complex chemical reactions initiated by UV irradiation, resulting in chain scission, formation of oxygen-containing functional groups, and progressive embrittlement of the material [6,7]. Since in recycled PP, these effects are exacerbated by the presence of pre-existing oxidative defects [8], maintaining adequate mechanical performance, particularly ductility and strength, over extended outdoor exposure remains a key challenge for the high-value reuse of rPP.

In a previous work, we demonstrated that a commercially available additive, namely Nexamite® R201 (NEX, an ethylene-based copolymer containing hydrolysable silicon groups), can modify the macromolecular architecture of recycled polyolefins [9]. In the specific case of rPP, the additive was found to partially restore the molecular weight lost during reprocessing while also promoting melt-structuring phenomena such as long-chain branching. These effects are particularly relevant for recycled PP, whose repeated processing history generally leads to chain scission, reduced melt strength, and poorer mechanical performance. Similar beneficial effects have also been reported for recycled high-density polyethylene, where Nexamite® R305 was shown to mitigate thermo-mechanical degradation during reprocessing [10]. Nevertheless, whether this molecular rebuilding strategy is also advantageous under subsequent service conditions, especially in the presence of UV radiation and moisture, remains unclear. In particular, the restoration of molecular weight and the introduction of new structural features may improve mechanical retention during aging, but they may also alter the oxidation pathway of the material.

On this basis, the present work was designed to address an important gap in the current literature concerning the durability of recycled polypropylene (rPP) under photo-oxidative conditions and the possible role of additives capable of restoring the molecular weight in improving its long-term performance. While a few studies on recycled polyolefins [11–14] have focused on reprocessing stability and re-stabilization through conventional antioxidant and UV-protection packages, the effect of additives specifically aimed at rebuilding the molecular architecture of rPP on its photo-oxidative degradation behavior has not yet been adequately clarified. Accordingly, the aim of the present work is twofold: first, to assess the photo-oxidative stability of a recycled polypropylene under accelerated weathering conditions, and second, to evaluate how the addition of a commercially available additive able to restore PP molecular weight after reprocessing affects the degradation behavior of the material. To this end, films of rPP and rPP modified with Nexamite® R201 were exposed to cyclic UVA irradiation and water condensation in a QUV apparatus, and the evolution of their morphology, chemical, thermal, rheological, and mechanical properties was systematically monitored. Particular attention was devoted to clarifying whether the additive, while beneficial in rebuilding the macromolecular architecture of reprocessed PP, can also preserve the mechanical integrity of the material during photo-oxidative aging. In this way, the study addresses a key question for the practical use of recycled PP in outdoor applications: whether molecular-weight-restoring additives can translate improved processability into improved durability in service.

2. Materials and Methods

2.1. Materials

The recycled polypropylene (rPP) employed in this study was collected from a recycling plant situated in Guarene (Cuneo, Italy). More specifically rPP was derived from post-consumer polypropylene trays. The recycled material was received in the form of flakes.

The additive Nexamite® R201 (NEX), composed of an ethylene copolymer comprising hydrolysable silicon-containing groups, was provided by Nexam Chemical (Lomma, Sweden). The amount of NEX added within rPP was 5 wt.%.

2.2. Processing

Cast-extruded films of rPP and rPP containing NEX (rPP+NEX) were obtained using a co-rotating twin-screw extruder (Process 11, ThermoFisher Scientific (Waltham, MA, USA)) equipped with 11 mm diameter screws (L/D = 40, screw profile already reported in a previous work [15]), a flat die (width: 25 mm, thickness: 1 mm), and a three-roll calendaring unit (Sheet Take Off for Process 11, Thermo Scientific (Waltham, MA, USA)). The processing conditions adopted during the film production were: flat temperature profile in the extruder at 200 °C, temperature in the flat die at 190 °C, feed rate of 500 g/h, and screw rotation speed of 200 rpm. The thickness of the produced films ranged from 320 to 380 μm.

2.3. Accelerated Weathering Test

In order to perform the accelerated weathering and evaluate the photo-oxidative degradation of pristine rPP and rPP+NEX, the QUV SOLAR EYE (Q-LAB, Westlake, OH, USA) was used. This instrument allowed us to expose the materials to controlled UV light and condensation conditions using fluorescent UV lamps with an irradiance equal to 0.77 W/m^2. The test conditions to which the films were subjected for their aging were the following:

- 8 h under UVA (365–295 nm) at 50 °C;
- 4 h of water condensation (100% relative humidity) with lamps switched off at 40 °C.

The films of rPP and rPP+NEX were put inside the QUV instrument after die-cutting them into ISO 527-5A [16] specimens. In order to record the changes induced by the photo-aging, the specimens were collected after a defined number of hours according to the intended characterisation. Each sample was named by designating at the end of the name the total time of aging; i.e., rPP t0 did not undergo any type of aging, and rPP t24 was collected after 24 h of aging.

2.4. Characterizations

Spectroscopical characterization was performed using a Frontier spectrophotometer (Perkin Elmer, Waltham, MA, USA) in two different configurations: reflection spectra of as-received pre-consumer rPP were acquired using a diamond attenuated total reflectance (ATR) accessory, while transmission spectra (FTIR) were carried out on the aged films collected from QUV every 24 h. The evolution of carbonyl groups (more specifically, carboxylic acid peak at 1712 cm^{-1}) was monitored to study the formation of oxidised species formed during the aging. The carbonyl index was then measured by normalizing the intensities of carbonyl group peaks with respect to the intensity of a reference peak (-CH- bending and stretching modes) at 2722 cm^{-1} [14,17]. For all measurements, 16 scans were collected at a spectral resolution of 4 cm^{-1}.

The thermal properties of the materials were characterized using a differential scanning calorimetry (DSC) TA Q20 (TA Instruments, Milford, MA, USA). The samples were subjected to a thermal cycle involving heating–cooling–heating runs in a nitrogen flow from 0 to 250 °C, with a heating/cooling rate of 10 °C/min. The crystallinity degree of the investigated materials was measured using the following equation:

$$\chi = \frac{\Delta H_m}{\Delta H_{m0}} \times 100, \quad (1)$$

where ΔH_m is the melting enthalpy (evaluated from the area of the melting peak), and ΔH_{m0} is the melting enthalpy of the 100% crystalline PP sample (207 J/g [18]).

The rheological behavior was evaluated using a strain-controlled ARES (TA Instruments, Milford, MA, USA) rotational rheometer. The measurements were performed under

nitrogen atmosphere using parallel plate (diameter: 25 mm) geometry. Preliminary strain sweep tests were carried out at 190 °C and at 10 rad/s to determine the linear viscoelastic region. Then, frequency sweep measurements were performed at 190 °C, in a frequency range of 10^2–10^{-1} rad/s. For each sample, the strain amplitude was selected to remain within the linear viscoelastic range.

The tensile tests on the specimens collected during the aging process were carried out at room temperature by using an Instron® (Norwood, MA, USA) 5966 testing machine. The instrument is equipped with 2 kN pneumatic grips and set to a gauge length of 50 mm. Five specimens were tested for every aging sampling, and the crosshead speed was set at 5 mm/min for all the tests. The tensile modulus, elongation at break and stress at break were determined, and their mean values (normalised with respect to the results obtained for the unaged samples) are reported as a function of the aging time.

3. Results

3.1. Preliminary Characterization of rPP

First of all, as-received recycled PP flakes (rPP) were characterised through spectroscopic and thermal analyses. The ATR-FTIR spectrum of rPP, reported in Figure 1, shows the characteristics peak of PP. In fact, according to the literature [19,20], the following signals can be recognised: (i) a peak at 2950 cm^{-1}, attributed to the asymmetric stretching vibration mode of -CH_3; (ii) a peak at 1375 cm^{-1} related to -CH_3 symmetric bending vibration mode; (iii) a peak at 1455 cm^{-1}, associated with -CH_3 asymmetric bending mode; and (iv) two peaks at 2838 and 2917 cm^{-1}, attributed to –CH_2– symmetric and asymmetric stretching, respectively. Therefore, from the analysis of the ATR-FTIR spectrum, it can be inferred that no other plastic contaminations are present in the rPP flakes. In addition, the broad band appearing in the range 1550–1750 cm^{-1} can be associated with the presence of carbonyl and vinyl products resulting from some thermo- and/or photo-oxidative degradation experienced by the polymer during its service life [21].

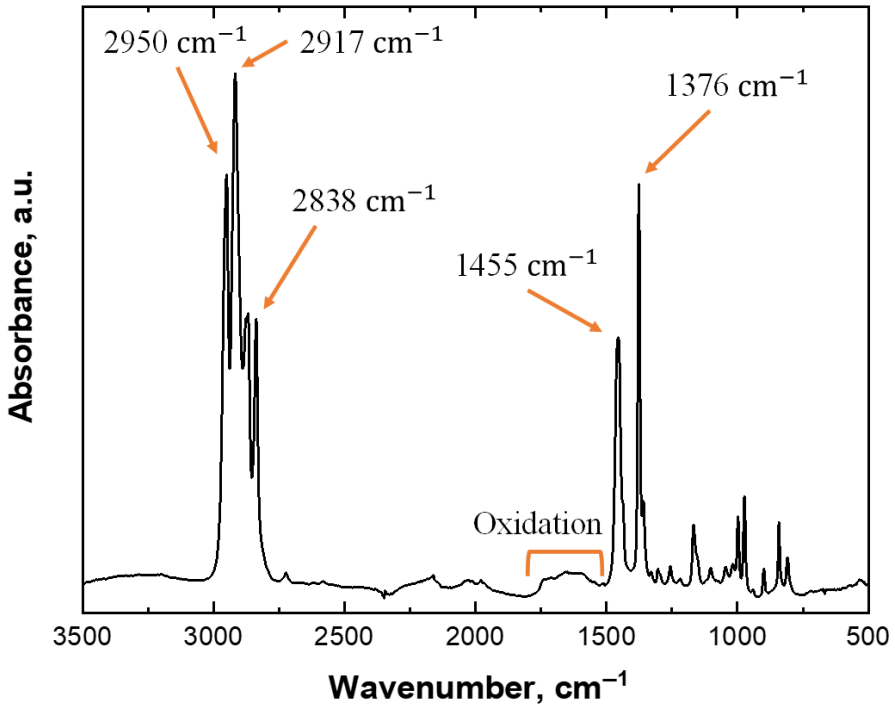

Figure 1. ATR spectrum of rPP flakes.

Concerning the characterization of the thermal properties carried out on as-received rPP flakes, the DSC analysis revealed an endothermic peak at about 165 °C recorded during heating, and an endothermic crystallisation peak during cooling at approximately 131 °C. According to the literature [22,23], these results are consistent with the presence of polypropylene as the sole polymeric component in the rPP flakes. Although the crystallization temperature is slightly higher than that typically observed for virgin PP, the recycled origin of the material investigated in this study should be taken into account. In particular, the presence of small amounts of contaminants, which may act as nucleating agents and thus promote crystallization, cannot be excluded [24].

3.2. Effect of NEX Introduction During the Processing

Frequency sweep tests were performed to assess the rheological behavior of the rPP flakes as received, after processing (rPP t0 film), and following the incorporation of NEX (rPP+NEX t0 film). Figure 2 reports the complex viscosity of all the investigated materials as a function of frequency.

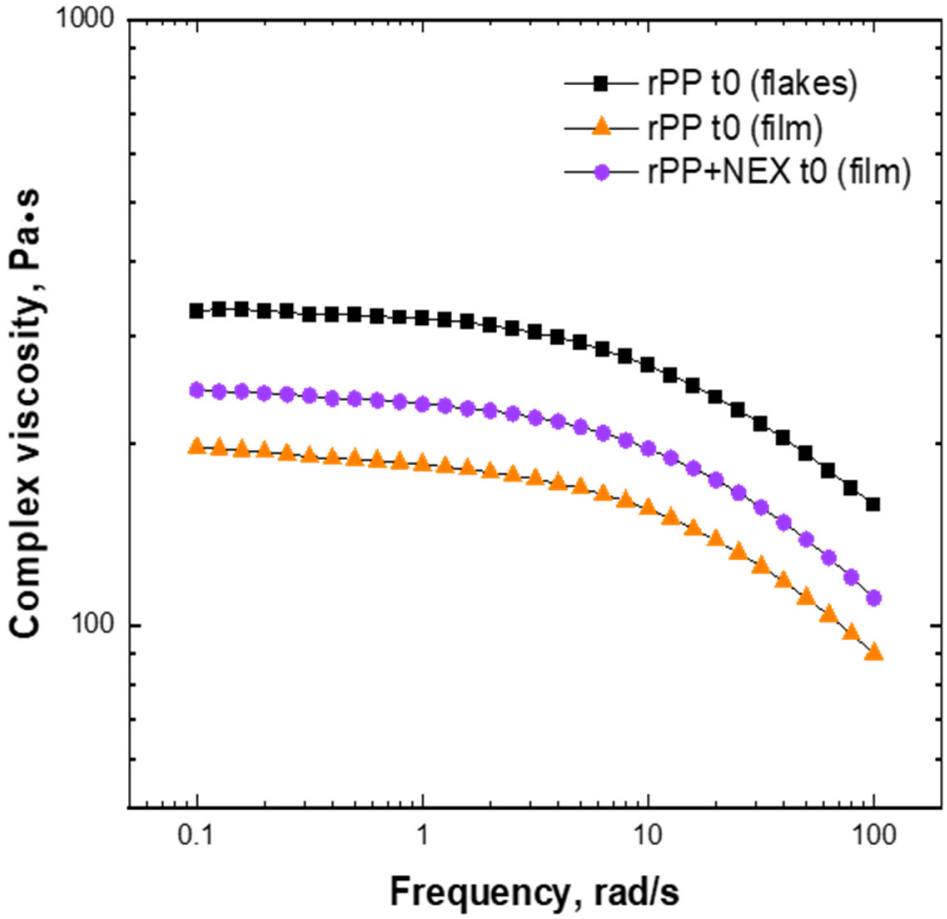

Figure 2. Complex viscosity curves of rPP as received (rPP t0 (flakes)) and after processing without (rPP t0 (film)) and with NEX (rPP+NEX t0 (film)).

All the curves show a pronounced Newtonian plateau at low and intermediate frequencies and a mild shear-thinning behavior at higher frequencies. Compared to the unprocessed rPP flakes, the cast-extruded film exhibits a decrease in complex viscosity across the entire investigated frequency range. This result can be ascribed to thermo-mechanical degradation phenomena occurring during processing, involving chain-scission reactions and the consequent reduction in molecular weight [22].

The effect of NEX addition is clearly apparent from the complex viscosity curves reported in Figure 2, which reveal an overall increase over the entire investigated frequency range. These results suggest that the additive enhances the complex viscosity, and thus the molecular weight, of rPP, although the original values of the as-received flakes are not fully recovered. This increase in viscosity is consistent with the findings of our previous study, where NEX was shown to partially restore the viscosity of a heavily degraded PP sample used to simulate the typical condition of a post-consumer recycled polymer [9]. In the present work, NEX was also found to be effective in rebuilding the molecular weight of a real post-consumer recycled PP.

3.3. Evolution of rPP+NEX Properties During the Aging Treatment

The rPP films, both without and with NEX, were then exposed to accelerated weathering in a QUV apparatus to investigate their behavior under photo-oxidative degradation in a moisture-containing environment. Throughout the aging treatment, the functional and structural characteristics of the films were monitored in order to evaluate the possible influence of the additive, and hence of the NEX-induced microstructural modifications, on the evolution of rPP properties and its long-term stability.

First of all, as observable in Figure 3, in the FTIR spectra of the aged materials (both with and without the additive), two new signals appear: a broad absorption band at around 3300–3600 cm^{-1} and a peak in the region between 1650 and 1800 cm^{-1}. Both signals can be attributed to the main products of the photo-oxidative degradation of PP, namely hydroperoxides and oxygen-containing groups, such as ketones, aldehydes, carboxylic acids, esters, and alcohols [6,25]. In particular, the first band can be associated with hydroxyl groups [26], while the peak centered at 1712 cm^{-1} is attributable to the formation of carbonyl group-containing species [27].

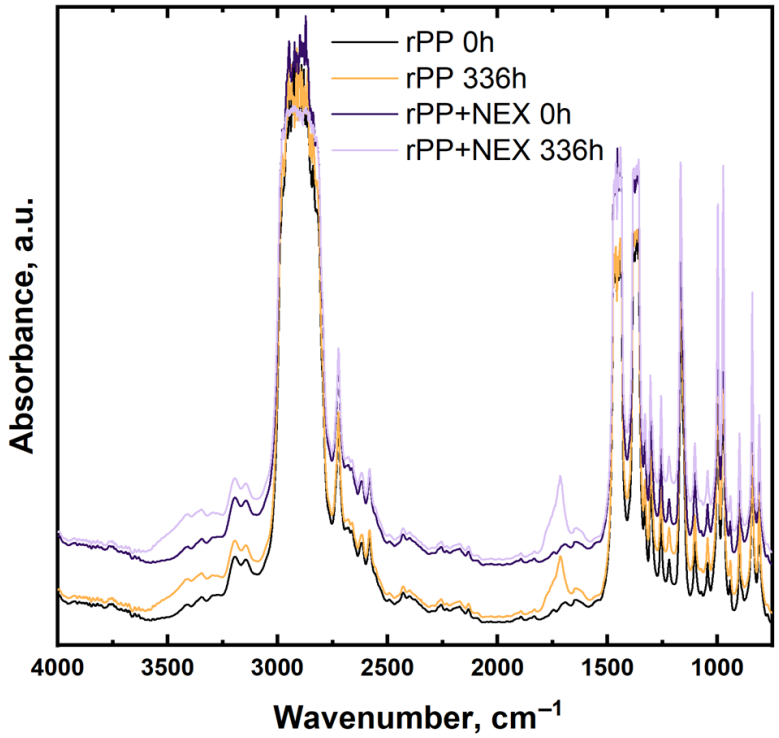

Figure 3. FTIR spectra of unaged and aged (336 h) rPP films, with and without NEX.

In order to monitor the progress of the photo-oxidation during the aging treatment, the evolution of the peak centered at 1712 cm^{-1} was followed. Figure 4a reports the trend

of the carbonyl index (calculated as the ratio between the intensity of the peak at 1712 cm^{-1} and that of a reference peak) as a function of the aging time.

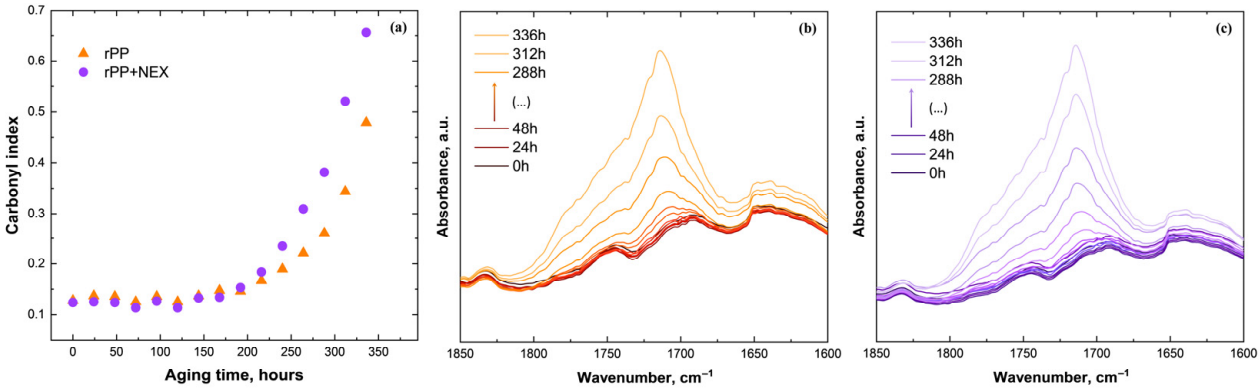

Figure 4. (**a**) Carbonyl index as a function of the aging time; Carbonyl band evolution as a function of aging time for (**b**) rPP and (**c**) rPP+NEX.

The carbonyl index exhibits the typical trend reported in the literature, namely an induction period followed by a growth stage [25], for both rPP and rPP+NEX. The non-zero values observed at 0 h indicate that a certain degree of photo-oxidative degradation was already present in the post-consumer rPP flakes before the aging treatment. As shown in Figure 4a, the carbonyl index remained nearly constant for both neat rPP and rPP+NEX from the beginning of the accelerated weathering up to approximately 200 h of aging. Beyond this point, both materials showed a progressive increase in the carbonyl index, although with different growth rates. In particular, the presence of the additive appeared to promote a faster formation of carboxylic acid species in aged rPP.

This behavior is also evident in the expanded FTIR spectra in the carbonyl region for rPP (Figure 4b) and rPP+NEX (Figure 4c). During the first 200 h of aging, all spectra substantially overlapped. Thereafter, an increase in the peak at 1712 cm^{-1} can be observed for both materials, although it is more pronounced in rPP containing NEX. This phenomenon may be explained by considering that the carbonyl group present in the additive can itself exert a photo-initiating effect through Norrish-type reactions [28]. Furthermore, a possible accelerating effect of the silicon-containing groups in NEX on the formation of carbonyl groups in rPP should also be taken into account, which likely also promotes the overall photo-oxidation process, as previously observed in polyolefin-based nanocomposites containing SiO_2 [6,27].

To evaluate the possible evolution of the thermal properties during aging, DSC analyses were carried out on rPP and rPP+NEX before the photo-oxidative treatment (t0) and after 96, 144, and 192 h of exposure. Figure 5 reports the DSC thermograms recorded during the first heating and cooling scans for all the investigated materials. Considering first the behavior of rPP without the additive, Figure 5a shows the evolution of the melting peak recorded during the first heating cycle. The melting temperature remained almost unchanged from the unaged sample up to 144 h of aging. However, after 192 h of exposure, changes in the shape of the melting peak and a decrease in melting temperature were observed. These phenomena can be associated with a reduction in lamellar thickness, leading to a broadening of the melting peak. In addition, the peak exhibited an irregular profile, and a second peak appeared, suggesting the formation of smaller crystallites as a consequence of prolonged aging [29]. In contrast, the crystallization temperature of rPP (Figure 5b) was not significantly affected by the aging treatment.

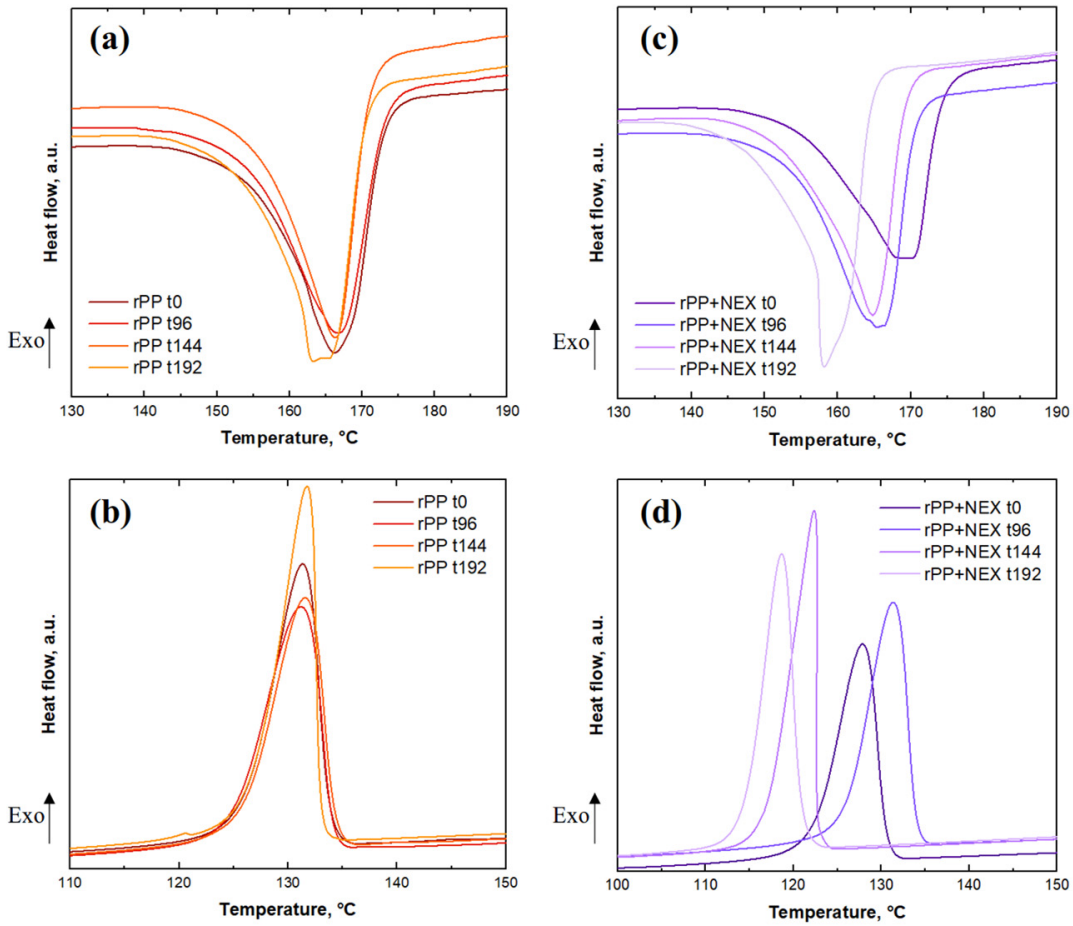

Figure 5. DSC thermograms recorded during the first heating and cooling scans for rPP (**a**,**b**) and rPP+NEX (**c**,**d**), respectively, at different aging times.

In contrast, the thermal properties of the system containing NEX showed marked changes with increasing aging time. As shown in Figure 5c,d, accelerated weathering induced more pronounced modifications in the thermal behavior of rPP when NEX was added prior to aging, compared with pristine rPP. As illustrated in Figure 5c, the shape of the melting peak also changed in this case, likely due to the formation of smaller crystallites with a reduced lamellar thickness, as discussed above. In addition, a progressive decrease in melting temperature was observed with increasing aging time. This behavior can be attributed to degradation occurring at the lamellar fold surfaces, involving the scission of tie molecules and an increase in the surface free energy of the crystals as a result of photo-oxidation reactions taking place at the crystal surface [28,30].

The crystallization temperature also exhibited significant variations with increasing aging time (Figure 5d), showing an initial increase followed by a decrease of more than 10 °C. This reduction can be associated with the accumulation of structural defects induced by photo-oxidative degradation [31], including the formation of oxygen-containing functional groups, the introduction of double bonds, and an increase in chain-end concentration. As a consequence, the crystals formed during cooling become smaller and more defective. Furthermore, the decrease in crystallization temperature may also be related to branching and/or crosslinking effects [32], in agreement with the macromolecular architecture previously inferred for rPP+NEX from the rheological analysis prior to aging.

Despite the observed variation in melting and crystallization temperatures, the crystallinity content (values reported in Table 1) remained almost unaffected by aging in both pristine rPP and rPP+NEX.

Table 1. Crystallinity content of rPP and rPP+NEX at different aging times.

	Crystallinity Content [%]	
Aging Time [h]	**rPP**	**rPP+NEX**
0	42	38
96	42	42
144	41	39
192	44	42

The mechanical properties as a function of the aging time were evaluated through tensile tests, and the mean values of elastic modulus, elongation at break and stress at break are reported in Figure 6. In order to better assess the variation in these properties as a function of the aging time, the tensile properties are reported in Figure 6 as normalized values, obtained by dividing the actual value of the property measured at a certain aging time by the value of the unaged sample.

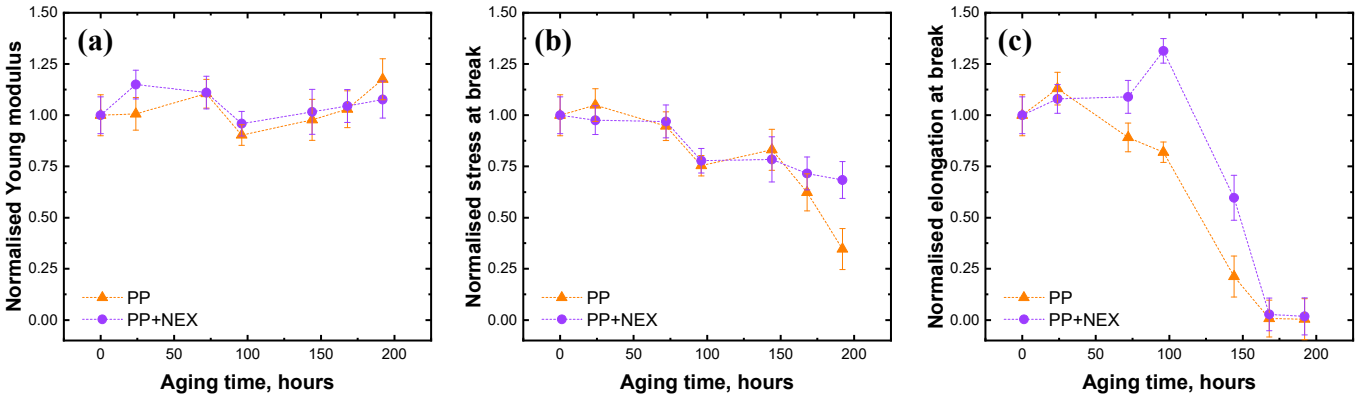

Figure 6. Normalised mechanical tensile properties of rPP and rPP+NEX as a function of the aging time: (**a**) elastic modulus, (**b**) stress at break and (**c**) elongation at break.

Evaluating how the tensile properties evolve during aging is of crucial importance to try to predict the material behavior before it becomes too fragile to withstand the application for which the films are intended. As widely reported in the literature, the typical effect of photo-oxidative degradation on polypropylene mechanical properties is an overall embrittlement of the material over time [31,33]. This is mainly due to chain scission phenomena occurring during photo-oxidative treatment, an increase in crystallinity and the formation of cracks on the surface of aged samples [29,34,35].

For both pristine rPP and rPP+NEX, the elastic modulus (Figure 6a) was only marginally affected by the aging treatment, with variations ranging from +18% to −10% of the initial value for rPP and from +15% to −4% for rPP+NEX over the investigated aging interval. In contrast, the stress at break (Figure 6b) progressively decreased with increasing exposure time. After 144 h of aging, both materials had lost approximately 20% of their initial value. However, whereas pristine rPP continued to exhibit a further reduction in stress at break at longer aging times, the NEX-containing sample showed a less pronounced decrease up to 144 h, followed by a total reduction of 32% after 192 h of exposure.

Figure 6c shows the trend of normalized elongation at break as a function of aging time. For pristine rPP, after a slight increase during the first 48 h of exposure, a marked decrease in ductility was observed with increasing aging time, and the sample displayed completely brittle behavior at the maximum exposure time, as also evidenced by the stress–strain curves reported in Figure 7. Interestingly, the addition of NEX promoted higher elongation-at-break values than those of the unaged sample, with a maximum

increase of 31% after 96 h of exposure. Beyond this point, the NEX-containing samples also exhibited a gradual decrease in elongation at break; however, after 144 h of aging, the reduction remained within 40% of the initial value, thus extending the exposure time over which the material could potentially be used in outdoor applications without undergoing severe embrittlement. At the end of the aging treatment, however, rPP+NEX also exhibited brittle characteristics, although with a different mechanical response to pristine rPP, as demonstrated by the stress–strain curves in Figure 7.

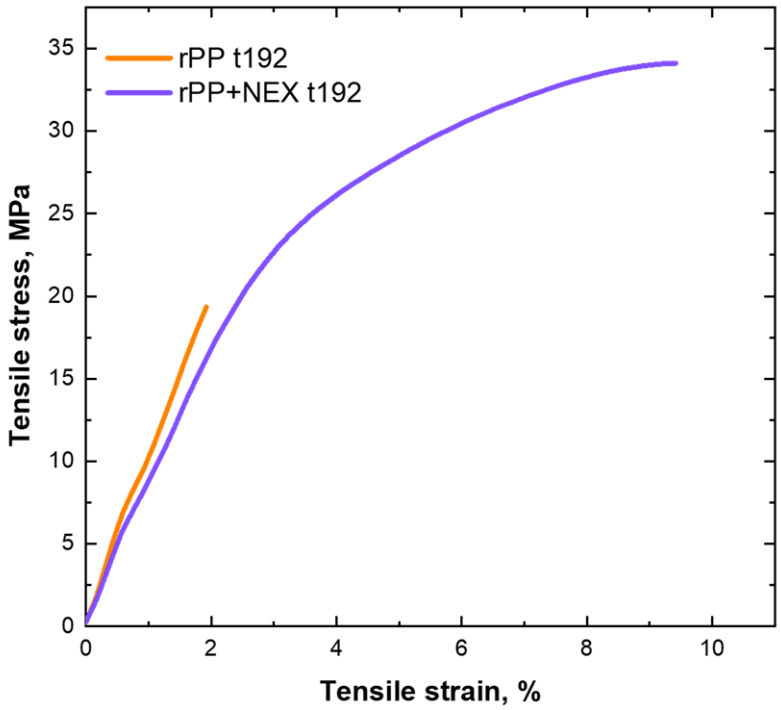

Figure 7. Tensile stress–strain curves of rPP and rPP+NEX aged for 192 h.

These findings are further supported by the SEM micrographs of the fracture surfaces after tensile testing for both samples at the maximum aging time reported in Figure 8. In particular, rPP exhibits a fully brittle fracture surface, whereas rPP+NEX shows a predominantly brittle morphology but still displays discernible signs of ductile fracture, demonstrating that, despite the overall brittle behavior, the material retains a residual degree of ductility.

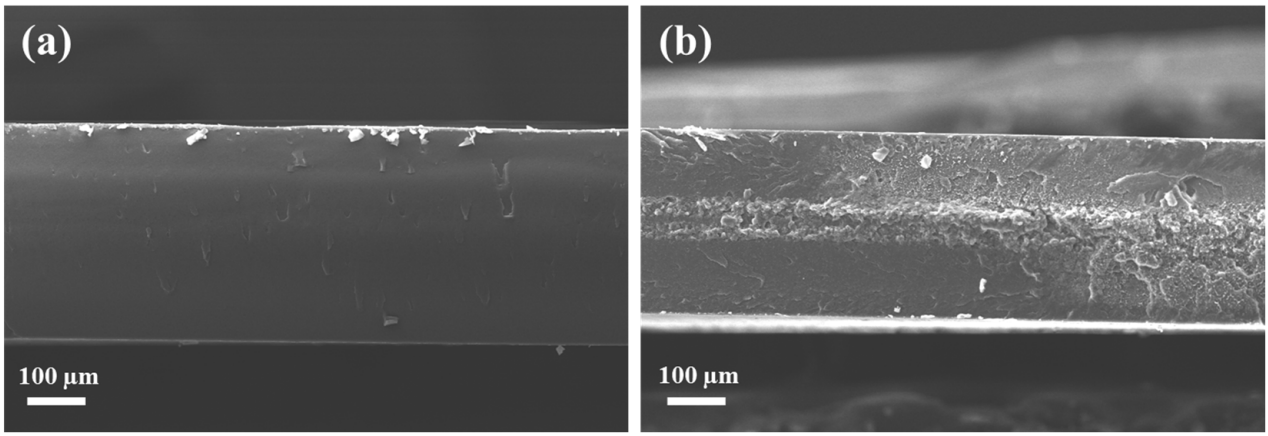

Figure 8. SEM micrographs of the fracture surfaces after the tensile tests for (**a**) rPP and (**b**) rPP+NEX aged for 192 h.

The observed behavior, namely the retention of higher elongation-at-break values during aging and the different evolution of stress at break, can be attributed to the microstructural modifications induced by NEX, even under photo-oxidative degradation conditions. A similar silicon-containing additive was used in one of our previous studies on recycled HDPE, where a marked increase in elongation at break was likewise observed [10]. In that case, the additive was found to direct the thermo-mechanical degradation reactions occurring during reprocessing toward the formation of long-chain branches, which in turn promoted the formation of tie molecules. The presence of tie molecules has been shown to enhance both elongation at break and tensile strength [36,37], owing to their role in stress transfer during tensile deformation [38]. Furthermore, tie molecules also play an important role in the recrystallization behavior of photo-oxidized PP, since chain scission and the sliding diffusion of tie molecules during aging can lead to the reorganization of crystalline domains and to the growth of thin lamellae [38]. Therefore, the higher elongation at break and stress at break observed in the NEX-containing sample may be ascribed to a rearrangement of the crystalline phases promoted by the presence of tie molecules, formed as a result of the melt-structuring effect induced by the additive, likely through the development of side branches. These findings are particularly relevant for the use of recycled PP in applications requiring prolonged exposure to outdoor environments. In such cases, the retention of mechanical performance over time is essential to ensure the effective use of recycled plastics and to enhance their circularity.

4. Conclusions

In this work, the effect of the commercially available additive Nexamite® R201 on the photo-oxidative aging behavior of recycled polypropylene films was investigated under accelerated UVA irradiation and water-condensation cycles. The results showed that both pristine rPP and rPP containing NEX underwent progressive oxidation, with functional degradation becoming evident after an induction period of about 200 h, as indicated by an increase in the carbonyl index. The higher oxidation rate observed for rPP+NEX suggests that the additive does not improve the chemical resistance of the material under the adopted weathering conditions. At the same time, the introduction of NEX significantly affected the structural evolution of the material during aging. In particular, DSC analysis revealed more pronounced changes in the melting and crystallization behavior of rPP+NEX than of neat rPP, indicating that the additive strongly influences the rearrangement of the crystalline phase during prolonged exposure. Despite this greater structural evolution and the faster buildup of oxidation products, the mechanical results highlighted a clear beneficial effect of the additive. In particular, NEX improved the retention of elongation at break and stress at break over extended aging times, thereby delaying the onset of severe embrittlement. Specifically, after about 150 h of exposure, the reduction in elongation at break was limited to about 40% in rPP+NEX, compared with nearly 80% in neat rPP, while after about 200 h, the loss in stress at break decreased from 65% for neat rPP to 32% for the NEX-containing system. This behavior is likely related to the macromolecular restructuring induced by the additive during reprocessing, which may promote the formation of branching and tie molecules, thus improving the ability of the material to retain load-bearing capacity during aging. Overall, the obtained results are promising for the development of recycled polypropylene materials intended for outdoor applications, where durability and retention of performance are essential for increasing the effective use and circularity of post-consumer plastics.

Author Contributions: Conceptualization, R.A. and A.F.; formal analysis, G.B. investigation, G.B.; data curation, R.A. and G.B.; writing—original draft preparation, G.B.; writing—review and editing, R.A. and A.F.; supervision, R.A. and A.F. All authors have read and agreed to the published version of the manuscript.

Funding: This study was carried out within the MICS (Made in Italy–Circular and Sustainable) Extended Partnership and received funding from the European Union Next-GenerationEU (PIANO NAZIONALE DI RIPRESA E RESILIENZA (PNRR)–MISSIONE 4 COMPONENTE 2, INVESTIMENTO 1.3–D.D. 1551.11-10-2022, PE00000004). This manuscript reflects only the authors' views and opinions, neither the European Union nor the European Commission can be considered responsible for them.

Institutional Review Board Statement: Not applicable.

Informed Consent Statement: Not applicable.

Data Availability Statement: The original contributions presented in this study are included in the article. Further inquiries can be directed to the corresponding author.

Acknowledgments: The authors want to acknowledge Nexam Chemical (Lomma, Sweden) for providing Nexamite® R201 and for the fruitful discussions.

Conflicts of Interest: The authors declare no conflicts of interest.

References

1. Schyns, Z.O.G.; Shaver, M.P. Mechanical Recycling of Packaging Plastics: A Review. *Macromol. Rapid Commun.* **2021**, *42*, 2000415. [CrossRef] [PubMed]
2. Jubinville, D.; Esmizadeh, E.; Saikrishnan, S.; Tzoganakis, C.; Mekonnen, T. A comprehensive review of global production and recycling methods of polyolefin (PO) based products and their post-recycling applications. *Sustain. Mater. Technol.* **2020**, *25*, 00188. [CrossRef]
3. Arese, M.; Bolliri, I.; Ciaccio, G.; Brunella, V. Post-Industrial Recycled Polypropylene for Automotive Application: Mechanical Properties After Thermal Ageing. *Processes* **2025**, *13*, 315. [CrossRef]
4. Raghuram, H.; Seier, M.; Koch, T.; Jones, M.P.; Archodoulaki, V.M. Smart design choices provide new applications for recycled polypropylene: The case for tribology. *Sustain. Mater. Technol.* **2023**, *38*, 00745. [CrossRef]
5. Westlie, A.H.; Chen, E.Y.; Holland, C.M.; Stahl, S.S.; Doyle, M.; Trenor, S.R.; Knauer, K.M. Polyolefin Innovations toward Circularity and Sustainable Alternatives. *Macromol. Rapid Commun.* **2022**, *43*, 2200492. [CrossRef]
6. Grause, G.; Chien, M.F.; Inoue, C. Changes during the weathering of polyolefins. *Polym. Degrad. Stab.* **2020**, *181*, 109364. [CrossRef]
7. Lv, Y.; Huang, Y.; Yang, J.; Kong, M.; Yang, H.; Zhao, J.; Li, G. Outdoor and accelerated laboratory weathering of polypropylene: A comparison and correlation study. *Polym. Degrad. Stab.* **2015**, *112*, 145–159. [CrossRef]
8. Gijsman, P.; Fiorio, R. Long term thermo-oxidative degradation and stabilization of polypropylene (PP) and the implications for its recyclability. *Polym. Degrad. Stab.* **2023**, *208*, 110260. [CrossRef]
9. Bernagozzi, G.; Arrigo, R.; Ponzielli, G.; Frache, A. Towards effective recycling routes for polypropylene: Influence of a repair additive on flow characteristics and processability. *Polym. Degrad. Stab.* **2024**, *223*, 110714. [CrossRef]
10. Bernagozzi, G.; Arrigo, R.; Frache, A. High Melt Strength Recycled High-Density Polyethylene: Evaluation of a Novel Route for Targeting the Polymer Microstructure. *Polymers* **2025**, *17*, 382. [CrossRef]
11. Mihelčič, M.; Oseli, A.; Huskić, M.; Slemenik Perše, L. Influence of Stabilization Additive on Rheological, Thermal and Mechanical Properties of Recycled Polypropylene. *Polymers* **2022**, *14*, 5438. [CrossRef]
12. Pfaendner, R. Restabilization – 30 years of research for quality improvement of recycled plastics review. *Polym. Degrad. Stab.* **2022**, *203*, 11082. [CrossRef]
13. Kouranou, D.; Galanopoulou, C.; Korres, D.M.; Tzani, A.; Detsi, A.; Vouyiouka, S. Restabilization of Post-Consumer Recycled Polypropylene with Natural Antioxidants from Spent Coffee Residue. *J. Appl. Polym. Sci.* **2025**, *142*, e56494. [CrossRef]
14. Delbruel, V.; Lajoie, H.; Steiner, V.; Gérard, J.F.; Duchet-Rumeau, J.; Chevalier, J. Effects of polypropylene compositions and processing conditions on its aging resistance under tropical environments. *Polym. Degrad. Stab.* **2024**, *228*, 110883. [CrossRef]
15. Lorenzi, E.; Arrigo, R.; Frache, A. Development of a Polypropylene-Based Material with Flame-Retardant Properties for 3D Printing. *Polymers* **2024**, *16*, 858. [CrossRef]
16. *ISO 527-1:2019*; Plastics-Determination of Tensile Properties-Part 1: General Principles. International Organization for Standardization: Geneva, Switzerland, 2019.
17. Xu, Z.; Tang, G.; Liu, Y.; Yang, R. Interfacial effects on photooxidative aging of silica-filled polypropylene composites. *Polym. Degrad. Stab.* **2024**, *227*, 110896. [CrossRef]
18. Kilic, A.; Jones, K.; Shim, E.; Pourdeyhimi, B. Surface crystallinity of meltspun isotactic polypropylene filaments. *Macromol. Res.* **2016**, *24*, 25–30. [CrossRef]

19. Caban, R. FTIR-ATR spectroscopic, thermal and microstructural studies on polypropylene-glass fiber composites. *J. Mol. Struct.* **2022**, *1264*, 133181. [CrossRef]
20. Morent, R.; De Geyter, N.; Leys, C.; Gengembre, L.; Payen, E. Comparison between XPS- and FTIR-analysis of plasma-treated polypropylene film surfaces. *Surf. Interface Anal.* **2008**, *40*, 597–600. [CrossRef]
21. Badini, C.; Ostrovskaya, O.; Bernagozzi, G.; Lanfranco, R.; Miranda, S. Recycling of Polypropylene Recovered from a Composting Plant: Mechanical Behavior of Compounds with Virgin Plastic. *Recycling* **2023**, *8*, 62. [CrossRef]
22. Spicker, C.; Rudolph, N.; Kühnert, I.; Aumnate, C. The use of rheological behavior to monitor the processing and service life properties of recycled polypropylene. *Food Packag. Shelf Life* **2019**, *19*, 174–183. [CrossRef]
23. Najafi, S.K.; Mostafazadeh-Marznaki, M.; Chaharmahali, M.; Tajvidi, M. Effect of Thermomechanical Degradation of Polypropylene on Mechanical Properties of Wood-Polypropylene Composites. *J. Compos. Mater.* **2009**, *43*, 2543–2554. [CrossRef]
24. Yakimets, I.; Lai, D.; Guigon, M. Effect of photo-oxidation cracks on behaviour of thick polypropylene samples. *Polym. Degrad. Stab.* **2004**, *86*, 59–67. [CrossRef]
25. Morlat, S.; Mailhot, B.; Gonzalez, D.; Gardette, J.L. Photo-oxidation of Polypropylene/Montmorillonite Nanocomposites. 1. Influence of Nanoclay and Compatibilizing Agent. *Chem. Mater.* **2004**, *16*, 377–383. [CrossRef]
26. Grigoriadou, I.; Paraskevopoulos, K.M.; Chrissafis, K.; Pavlidou, E.; Stamkopoulos, T.G.; Bikiaris, D. Effect of different nanoparticles on HDPE UV stability. *Polym. Degrad. Stab.* **2011**, *96*, 151–163. [CrossRef]
27. Lu, M.; Gao, X.; Liu, P.; Tang, H.; Wang, F.; Ding, Y.; Zhang, S.; Yang, M. Photo- and thermo-oxidative aging of polypropylene filled with surface modified fumed nanosilica. *Compos. Commun.* **2017**, *3*, 51–58. [CrossRef]
28. Li, J.; Yang, R.; Yu, J.; Liu, Y. Natural photo-aging degradation of polypropylene nanocomposites. *Polym. Degrad. Stab.* **2008**, *93*, 84–89. [CrossRef]
29. Seldén, R.; Nyström, B.; Långström, R. UV aging of poly(propylene)/wood-fiber composites. *Polym. Compos.* **2004**, *25*, 543–553. [CrossRef]
30. Ojeda, T.; Freitas, A.; Birck, K.; Dalmolin, E.; Jacques, R.; Bento, F.; Camargo, F. Degradability of linear polyolefins under natural weathering. *Polym. Degrad. Stab.* **2011**, *96*, 703–707. [CrossRef]
31. Dahal, P.; Kim, J.H.; Kim, Y.C. Effects of linear low-density polyethylene on physical properties and irradiation effectiveness of polypropylene. *Korean J. Chem. Eng.* **2014**, *31*, 1–5. [CrossRef]
32. La Mantia, F.P.; Baiamonte, M.; Santangelo, S.; Scaffaro, R.; Mistretta, M.C. Influence of Different Environments and Temperatures on the Photo-Oxidation Behaviour of the Polypropylene. *Polymers* **2022**, *15*, 74. [CrossRef]
33. Rabello, M.S.; White, J.R. Crystallization and melting behaviour of photodegraded polypropylene—I. Chemi-crystallization. *Polymer* **1997**, *38*, 6379–6387. [CrossRef]
34. Rouillon, C.; Bussiere, P.O.; Desnoux, E.; Collin, S.; Vial, C.; Therias, S.; Gardette, J.L. Is carbonyl index a quantitative probe to monitor polypropylene photodegradation? *Polym. Degrad. Stab.* **2016**, *128*, 200–208. [CrossRef]
35. Park, S.J.; Lim, H.K.; Lee, S.J.; Im, S.H.; Lee, J.; Jung, Y.; Kim, S.H.; Shim, J.S.; Won, J.; Chung, J.J.; et al. Enhancing Biodegradable Bone Plate Performance: Stereocomplex Polylactic Acid for Improved Mechanical Properties and Near-Infrared Transparency. *Biomacromolecules* **2025**, *26*, 2390–2401. [CrossRef]
36. Long, C.; Dong, Z.; Wang, K.; Yu, F.; He, C.; Chen, Z.R. Molecular weight distribution shape approach for simultaneously enhancing the stiffness, ductility and strength of isotropic semicrystalline polymers based on linear unimodal and bimodal polyethylenes. *Polymer* **2023**, *275*, 125936. [CrossRef]
37. Nitta, K.H.; Takayanagi, M. Role of tie molecules in the yielding deformation of isotactic polypropylene. *J. Polym. Sci. Part. B Polym. Phys.* **1999**, *37*, 357–368. [CrossRef]
38. Dudic, D.; Kostoski, D.; Djokovic, V.; Stojanovic, Z. Recrystallization processes induced by accelerated ageing in isotactic polypropylene of different morphologies. *Polym. Degrad. Stab.* **2000**, *67*, 233–237. [CrossRef]